

PLENARY REPORT

ELECTRON BEAM WELDING - PROCESS AND TECHNIQUES

Peter Petrov

Institute of Electronics, BAS, Tsarigradsko Chaussee 72, 1784 Sofia, Bulgaria

Electron beam welding, is still widely used in industry such as automotive, aerospace, nuclear, electrical engineering etc. The electron beam technology ensures welded joints a wide range of thickness from 0.02 mm to 300 mm and also for production of films and coatings by deposition and surface modification of the metals and alloys. In this paper we are focused on the process and techniques during electron beam welding.

Key words: electron beam welding, techniques

INTRODUCTION

The electric arc had been known as a physical phenomenon for decades without practical application, until the Russian inventor N. N. Benardos (1842-1905) found that it could be used for joining of metallic parts. In 1885 Benardos obtained a patent for carbon arc welding. The method was further developed by N. G. Slavyanov, who replaced the carbon electrode by consumable metal electrode. At that time the process was difficult to operate, since the arc between the metal electrode and the processed workpiece was unstable and this complicated the regulation of the metal transfer from the electrode to the weld. The introduced by Oscar Kjellberg in 1905 electrodes with covering and their improvement revolutionized the process of electric arc welding with metal electrode. The covering made the arc much more stable and improved the transfer of molten metal drops, leading to a much enhanced quality of the weld metal. The covered electrodes used presently in the manual electric arc welding are based on the same principles. In parallel with arc welding, the resistance welding was developed and in 1886 E. Thomson obtained a patent for this process [1].

A significant improvement in the welding technology was realized after the mid-fifties of the past century, when the welding machinery producers were competing in using the latest achievements in science and technology. Today's more than 200 modifications of the welding technologies are so advanced that the quality standards are easily met. The latest trends in the welding technologies concern both the development of novel welding sources and materials, and the implementation of computer-based models for further optimization of the manufacturing process. An example is the **electron beam welding** (EBW), which has been industrially applied since the seventies of the last century.

EXPOSITION

Electron beam welding process

The EBW welding is characterized by two main ranges of the density of the energy introduced. The first one, with power densities q up to 10^6 W/cm², where a molten zone with an almost spherical shape is formed; the second one, with q exceeding 10^6 W/cm², is characterized by the deep melting effect with the appearance of a keyhole in the molten pool. During welding, the keyhole moves

together with the electron beam thus determining the shape and size of the welding seam. The electron beam welding with key-hole cavity produce the typical needle-like weld profile. The width-to-depth ratio of the weld reaches 1:30 and more. The welding power and speed determine the shape and size of the weld. EBW processes allow for high welding speeds and high level of technological automatization. The main advantage of the

electron beam welding is that due to the high energy density in the workpiece, the total energy introduced in the material for welding a certain section is several times less as compared to the conventional methods (arc, argon shielded, plasma, etc.). This determines the much lower heat influence of the welding process on the heat affected zone and the weld [1-3].

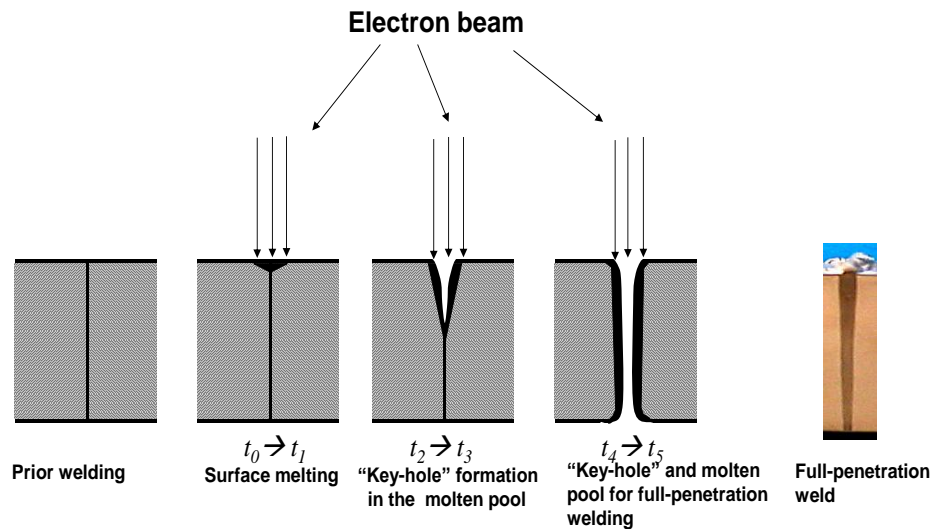


Fig. 1. The kinetics of molten pool and cross-section of full penetration weld

The kinetics of molten pool during EBW formation is schematically presented in Fig.1 [4]. At the initial moment t_0 the electron beam reaches the cold metal surface at normal incidence. The electrons penetrate a small depth, heating the surface layer. At a certain temperature (different for the different materials) the metal starts evaporating and molten phase is formed. In the figure this corresponds to the time interval t_0-t_1 . As the temperature increases, and as a result of the vapour pressure, the so called keyhole is formed in the molten pool. This takes place during the time interval t_2-t_3 (or t_4-t_5 in the case of full penetration welding). The keyhole profile is asymmetric – the molten metal layer at the front wall is thinner than at the back wall (taken with respect to the direction of motion of the workpiece) Fig.2a.

Several approaches have been developed to analyze the causes and conditions of keyhole formation in the molten pool EBW. According to the first one, proposed by

Schwarz [5], the material in the interaction zone is melted and vaporized, which results in the appearance of a keyhole whose surface is covered by a thin layer of molten metal. Tong and Gied [6] suggested that the main cause of keyhole formation is the vapor pressure forces acting during metal evaporation in the molten pool. Another approach, developed by Rykalin and co-authors [2], is based on the explosive boiling of the molten metal as a result of the rate of heat introduction exceeding that of heat dissipation by heat conduction in the zone of electron-beam interaction with the material. The appearance during EBW of non-equilibrium plasma with high particle density causing scattering and subsequent focusing of the electron beam lies in the basis of the hypothesis [7] stating that, thanks to the processes of ion focusing, the electron-beam diameter decreases by a factor of 10 or more, due to which the keyhole shape and size change with time.

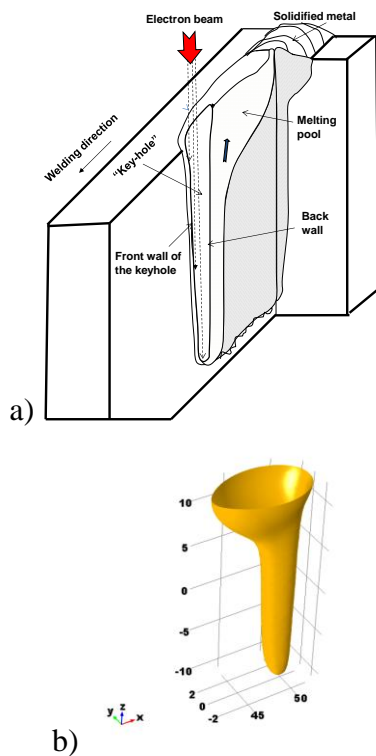


Fig. 2. a) Scheme of the: electron beam welding seam formation; b) melting pool

During the electron beam welding process, the molten pool Fig. 2.b is in an unstable equilibrium. There are two main streams of molten metal from the melting front to the solidification front: horizontal – around the keyhole and vertical – first towards the bottom of the pool and then up its back wall. The liquid phase quantity is minimal at the pool bottom. There the electron beam interacts with the solid metal and most probably the irregularities in the lower part of the molten zone are connected with the change in the electron beam configuration after scattering in the vapour phase. The mass transfer from the front to the back wall of the keyhole is realized mostly along the walls in horizontal direction, while transfer through the pool bottom is rather unlikely. The molten metal moves downwards along the front wall until filling the entire depth of the keyhole, and this is repeated periodically. These fillings prevent the transportation of metal through the bottom of the molten pool. The vertical mass transfer along the back wall is predominant, so the molten part of the zone (near the surface) is much wider than the middle and the lower parts [8-10].

1. Electron beam welding equipment

The general scheme of the EBW installation is shown in Fig.3. The electron generation, acceleration and focusing is realized in an electron beam generator (EBG). The electrons are emitted from a heated tungsten electrode in the electrostatic part of the electron gun Fig.4.a. In triode guns, the control of the electron beam current is realized by varying the potential of the control electrode (wehnelt) up to 3 kV at constant accelerating voltage Fig.4.b [9,10]. The electrons emitted by the cathode are accelerated in the potential difference between the cathode and anode, which is from 40 to 150 kV. The minimal cross-section of the electron beam after the emitter, obtained due to its focusing by the electrostatic field, is called crossover. After the crossover plane, the electron beam expands and has a conical shape. Then the beam is focused again by the electromagnetic system consisting of a cylindrical coil with an external armco core. Variation in the coil current I_f changes the magnetic field, and the convergence angle of the electron trajectories, thus controlling the electron beam.

Additionally, the EBW installation includes low voltage power supplies for the focusing, deflection and alignment systems of the electron gun.

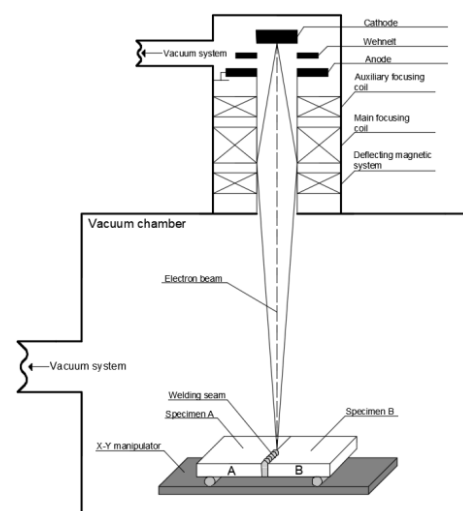


Fig. 3. Scheme of the electron beam welding machine

The EBG is fixed to a high vacuum work chamber, where the welding process

takes place. An XYZ manipulator in the work chamber provides the positioning of the components to be welded. The chamber volume depends on the size of the welded workpieces. The chamber walls provide the necessary mechanical strength, vacuum sealing and protection against the X-rays formed during the interaction of the accelerated electrons with the welded material. The high vacuum maintained in the work chamber requires the use of a vacuum system consisting of high vacuum diffusion pumps, turbo-molecular and mechanical fore-vacuum pumps, as well as vacuum valves, pipes and measurement devices. For efficient electron beam welding, the vacuum system should provide a working pressure of 1.33×10^{-3} Pa to 1.33×10^{-5} Pa in the electro-optical system and 1 Pa to 10^{-3} Pa in the work chamber.

The electron beam is aligned to the

welding gap, and the workpieces are positioned by means of the XYZ manipulator. The electromagnetic deflection system scans the electron beam over the gap both in transverse and in longitudinal direction. In the state of the art installations, the vacuum system, the XYZ manipulator and the technological parameters of the electron beam welding (accelerating voltage, electron beam current, focusing system current) are microprocessor controlled. The entire welding process is monitored with the help of optical and CCD systems.

The main parameters of the welding electron beam are the size of the beam cross-section, the convergence (divergence) angle θ , and the position of the focal plane (the cross-section where the beam diameter d_b is minimal) with respect to the surface of the welded workpiece (Fig.4c).

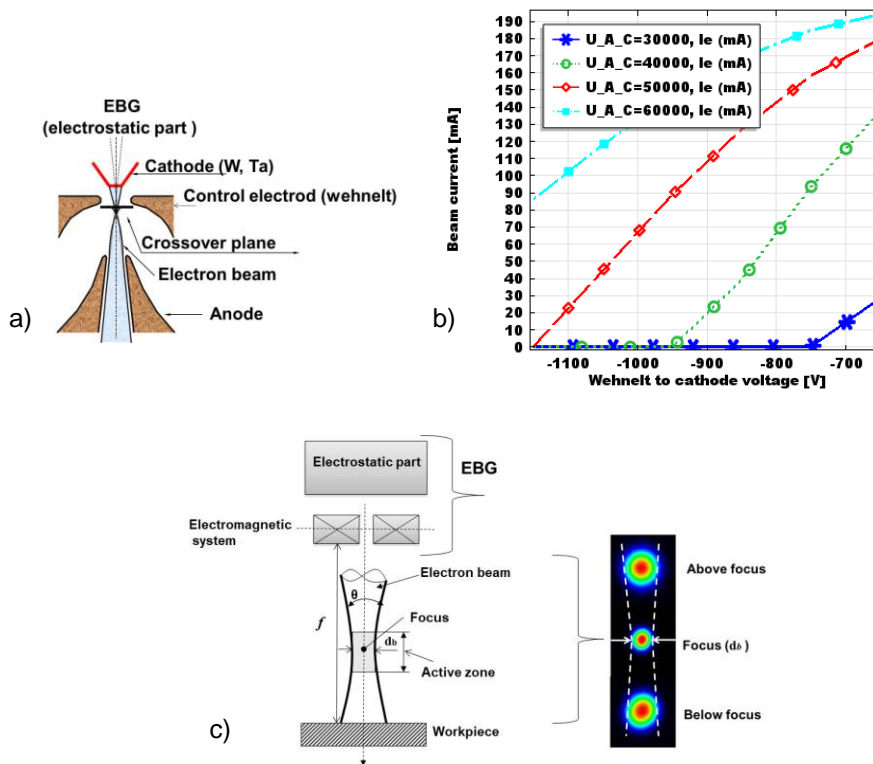


Fig. 4. a) Electrostatic part of the electron gun; b) electron beam current vs. wehnelt to cathode voltage; c) scheme of the electron beam focus position;

The energy density, or intensity, of the heat source q_2 (W/m^2) is defined as:

$$q_2 = UI/A \quad (1)$$

where: U is the accelerating voltage,

[V]; I is the electron beam current [A], $A = \pi d^2/4$ is the surface area of the focused beam on the surface of the workpiece, [m^2]; d is the electron beam diameter [m].

The electron beam diameter in the focal plane d depends on the electron beam current I and the accelerating voltage U and is determined as:

$$d = S_0 \left(\frac{I}{U} \right)^{\frac{3}{8}} \quad (2)$$

where

$S_0 = \left(4^{2/3k} / \pi e C^{2/3} f^{2/3T} / j \right)^{\frac{3}{8}}$; is a constant, characterizing the electro-optical system "electron gun"; T is the cathode temperature [K]; $e = 1.6 \cdot 10^{-19} \text{C}$; k is the Boltzmann constant [J/K]; C is a dimensionless constant of the spherical aberration of the electromagnetic lens; j is the current density for cathode thermo-electron emission [A/cm^2]; f is the focal distance [cm];

Thus Eq. 1 can be re-written as:

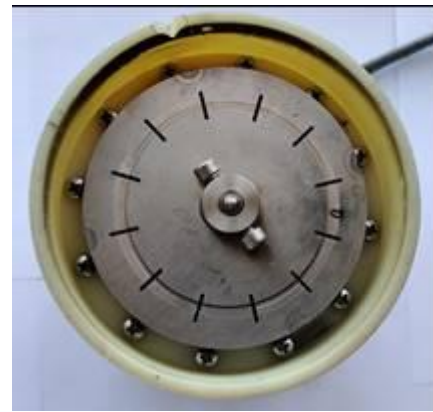
$$q_2 = \frac{1}{\pi} \left(\frac{2}{S_n} \right)^2 I^{1/4} U^{7/4} \quad (3)$$

4

The part of the electron beam where the heat source intensity q_2 (W/cm^2) is higher than a critical value q_{cr} is called „active zone“ (Fig.4c). The critical value of the power density is generally defined as the value which leads to a needle-shaped weld and a keyhole in the molten pool.

The quality of the weld depends on the active zone profile and position with respect to the welded workpiece. In practice the active zone size is usually determined using a special sample, placed at 300 with respect to the welding plane. This test is known in literature as Arata Beam Test [2]. The power density, and thus the active zone size and the electron beam diameter d_b , can be varied by means of the electromagnetic focusing system. The maximal power density is limited due to the electron beam spatial charge distribution.

A device (electron beam analyser) is developed to measure the diameter of the electron beam [13]. This equipment is based on a rotating disc with multiple slits in it Fig.5a. The disc is turning at high speed (up to 3500 rpm) and signal from electron beam is registered from an oscilloscope Fig.5b.



a)



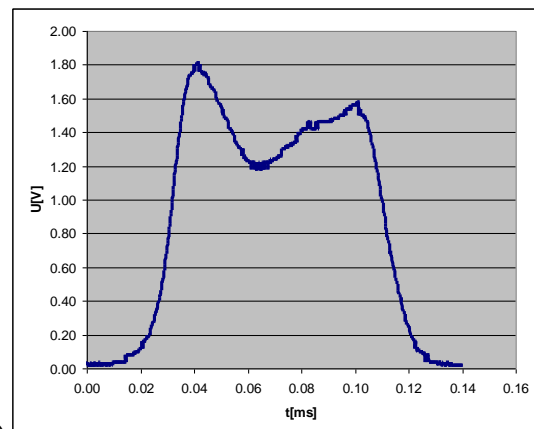
b)

Fig. 5. Electron beam chopper device a); Sample signal from an oscilloscope b).

The electron beam diameter can be calculated using the law of uniform motion:

$$d = t_p v - \delta \quad (4)$$

where d is the electron beam diameter, v is the velocity of the disc at the point where the beam is falling, t_p is the duration of a single impulse and δ is the width of a slit Fig.6a.



a)

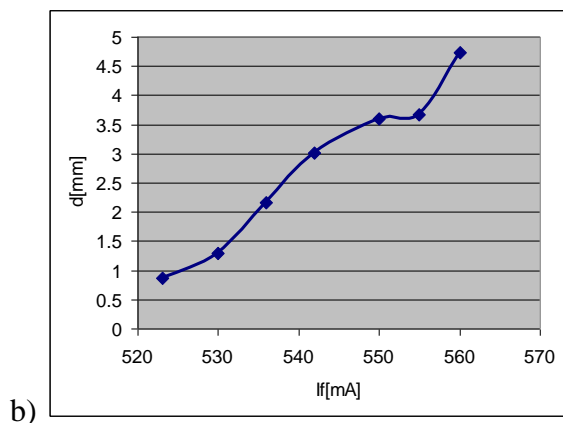


Fig. 6. Duration of a single impulse a); Diameter of the electron beam vs focusing current b)

The velocity is calculated from the time needed for the disc to turn from one slit to the next via the equation;

$$v = \delta * r / (\pi * T) \quad (5)$$

where r is the measured distance between the center of the disc and the falling of the beam ($r=37$ [mm]), T is the time between the start of two consecutive peaks, and $\pi/6$ is the angle between two consecutive slits in radians. The calculated electron beam diameters with respect to the focusing current are shown in Fig. 6b.

CONCLUSION

The processes taking place during electron beam welding at electron-beam power density $\geq 10^6$ W/cm² can be summarized as follows: (i) the electron-beam energy is distributed along the depth of the keyhole in the molten pool, which is predominantly due both to the processes of electron-beam scattering in the metal vapors, and to those of heat- and mass-transfer in the keyhole and the molten pool as well; (ii) the quality of the weld depends on the active zone profile and position with respect to the welded workpiece; (iii) the power density, and thus the active zone size and the electron beam diameter, can be varied by means of the electromagnetic focusing system. The maximal power density is limited due to the electron beam spatial charge distribution.

Acknowledgements

This work was supported by the Project of OP „Science and Education for Smart Growth "Creation and development of centres of competence"

BG05M2OP001–1.002–0023–C01

"INTELLIGENT MECHATRONICS, ECO-AND ENERGY-SAVING SYSTEMS AND TECHNOLOGIES" (IMEEST)

REFERENCE

- [1] V. Mihailov, V. Karhin, P. Petrov, Fundamentals of welding (In English), Polytechnic University Publishing St. Petersburg, 2016, pp 283 ISBN 978-5-7422-5569
- [2] Y. Arata "Plasma, Electron and Laser Beam Technology" American Society for Metals, (1986) 630 pages.
- [3] N.N. Rykalin, A.A. Uglov, A.G. Zuev, A.N. Kokora, "Laser and electron-beam treatment of materials", Moscow, Mashinostroene Publishers, (1985) 495 pages (in Russian).
- [4] P. Petrov, Ch. Georgiev and G. Petrov "Experimental investigation of weld pool formation in electron beam welding" Vacuum, Vol.51, n. 3(1998)339-343.
- [5] H. Schwarz, J Appl. Phys, V 35, n.7, (1964)2020.
- [6] H. Tong, W. Gied, Welding J, V. 49, n.6, (1970)259.
- [7] V. Ledovskoy, G. Mladenov, Russian Journal of Technical Physics, v. 11 (1970) 2260 (in Russian).
- [8] Stefanov B., P. Petrov, Pirgov P., "Electron beam evaporation and welding: plasma formation and liquid pool instabilities" Vacuum, v.38, n.11,(1988)1029-1033.
- [9] P. Petrov, M. Tongov, Numerical modelling of heat source during electron beam welding, Vacuum 171 (2020) 108991, <https://doi.org/10.1016/j.vacuum.2019.108991>
- [10] P. Petrov, M Tongov, Study of the cathode emissivity in generators for electron beam systems, Optik, Volume 209, May 2020, 164358, <https://doi.org/10.1016/j.ijleo.2020.164358>
- [11] P. Petrov, M. Tongov, M. Ormanova, S. Valkov, Study of the processes in the electrostatic part of the electron-beam generator, Comptes rendus de l'Académie bulgare des Science, Vol 73, No 9, (2020)1225-1228
- [12] M. Tongov, T. Hikov, I. Angelov, P. Petrov, Measuring the diameter of electron beam by rotating slit disc, IOP Conf. Series: Materials Science and Engineering 878 (2020) 012053, doi:10.1088/1757-899X/878/1/012053